



## Effect of Solar Air Flat Plate Collector Geometric Parameters on The Thermal Behavior Inside an Indirect Solar Drier

Open  
Access

Daoud Halassa<sup>1</sup>, Mohamed Announ<sup>1</sup>, Abdelghani Boubekri<sup>2,\*</sup>, Djamel Mennouche<sup>3</sup>, Hamza Bouguettaia<sup>3</sup>

<sup>1</sup> Laboratoire Matériaux et Environnement, Faculté de Technologie, Université Yahia FARES de Médéa, Algérie

<sup>2</sup> Laboratoire de développement des énergies nouvelles et renouvelables en zones arides et sahariennes, Université Kasdi Merbah Ouargla, Algérie

<sup>3</sup> Département de génie mécanique, Faculté des sciences appliquées, Université Kasdi Merbah Ouargla, Algérie

### ARTICLE INFO

### ABSTRACT

#### Article history:

Received 19 April 2019

Received in revised form 15 July 2019

Accepted 23 September 2019

Available online 29 September 2019

This work focuses on the possibility of determining the most efficient type of solar air flat plate collector (simple pass or double pass collector) as well as examining the effect of its geometric parameters in order to achieve a good homogeneity of the temperature distributed inside the indirect solar drier which is naturally ventilated. Several investigations conducted experimentally show a more elevated efficiency by 8% of the simple pass collector in comparison with the double pass collector. A CFD simulation, which was done based on variations in the length and width of the solar collector under different climatic conditions, reveals that the 4m x 1.5m solar simple pass collector produces a more homogenous distribution of temperature which is better suited for the drying system.

#### Keywords:

Solar drying; solar air collector; thermal efficiency; natural ventilation; geometric design

Copyright © 2019 PENERBIT AKADEMIA BARU - All rights reserved

## 1. Introduction

Nowadays, the drying process is widely used in the food industry and attracts a lot of researchers' attention for the purpose of preserving crops for a long time by reducing their water content through evaporation [1-2] resulting in inhibiting micro-organisms growth and enzymatic actions which cause them to rot [3, 4]. A large variety of crops, grown in North Africa such as tomatoes, apricots, potatoes, dates and mint, could be dried off in order to be preserved for consumption. Moreover, there is a growing interest worldwide in dry foods because it does not require a large storage space and could also be transported at very low cost [5, 6]. Therefore, over the last few years, the Algerian Government has launched a promising program to incentivize the business community to make bigger investments in local agriculture which seems to be a better substitute for the petroleum industry whose earnings continue to dwindle, and since there is a tremendous amount of solar

\* Corresponding author.

E-mail address: [boubekri.abdelghani@univ-ouargla.dz](mailto:boubekri.abdelghani@univ-ouargla.dz) (Abdelghani Boubekri)

radiation available over a long period in the Sahara, many cheap solar-drying equipment and techniques could be exploited to make the food industry more efficient and profitable [7].

Several studies have been carried out by many researchers to make improvements on both the design of the solar-drying equipment, and the operating conditions to obtain the best quality possible of dry foods and medicinal products [8,9]. These improvements were made based on both experimental and numerical approaches. Suhaimi Misha *et al.*, [10] designed an industrial scale tray dryer for chipped kenaf core. By using a CFD method they studied the airflow distribution in the drying chamber to ensure drying uniformity. Uniform airflow distribution in a drying chamber is very important because it strongly influences the dryer efficiency and homogeneity of the products being dried. The air collector is a central part of the solar drying system of food for two essential reasons: Firstly, because it is used as a source of hot air which circulates inside the drying chamber. Secondly, it makes it possible to obtain a high quality of dry products without any flaws deterioration [11-13]. It is worth mentioning that the performance of the drying system largely depends on both the geometric design and the thermal behavior of the collector which has become the main subject of many research projects attempting to enhance its efficiency [14,15]. Suwasti [16] investigated experimentally the influence of the collector design on the performance of the solar dryer under natural convection conditions. Karim and Hawlader [17] conducted an experimental study based on the ASHRAE standard using three types of solar air collectors: flat plate, finned and v-corrugated in order to examine the efficiency of the solar drier over a wide range of operating and design conditions under Singapore climatic conditions. An experimental investigation conducted by Babahani *et al.*, [18] on an unventilated indirect solar dryer, designed and manufactured by Energy conversion research group at "LENREZA laboratory, Ouargla University in Algeria", shows that the dried product is marked by a tanning phenomenon, and even some burns in areas close to the walls of the drying chamber. These observations can be attributed to both the non-homogeneity of the temperature distributed and the air emanating from the solar air collector and flowing out through the chimney. The root-cause of this phenomenon could be the combination of the following factors or just one of them: the geometric configuration of the drying chamber, the air collector and the exit of air through the chimney. They have suggested a solution for these problems based on an assumption related to the geometric configuration H/L of the drying chamber and have experimentally examined the solar dryer with and without product to check the distribution of temperature in the drying chamber. The results of this study confirm the presence of a thermal stratification phenomenon close to the exit of the chimney due to the lack of temperature homogeneity mainly when the products are high in moisture content.

It is worth noting that not many studies have been carried out on the thermal and dynamic aspects of the solar collector connected with the drying chamber, and most of them are indeed done in an attempt to improve its efficiency. Therefore, the combination of experimental data with a numerical simulation makes it possible to analyze accurately the thermal transfer phenomena in the drying system (solar collector and drying chamber). The main purpose of this paper is not only to determine the most efficient type of collector (simple pass or double pass), but also to investigate both the influence and contribution of the geometric parameters of the collector that could produce more homogeneous distribution of temperature inside the drying chamber under different climatic conditions in the Saharan city of Ouargla, south east of Algeria, where the experiment was exactly conducted.

## 2. Materials and Methods

### 2.1 Experimental Set-Up and Procedures

The city of Ouargla is actually characterized by a dry and hot climate. The wind speed varies on average from 2.0 m/s to 4.3 m/s [19]. The abundance of both solar radiation and high temperature all year long makes the city of Ouargla a good place for the installation of drying system. A typical example of a daily solar radiation and the variations in ambient temperature (May 2015) in this city are illustrated in Figure 1.

The prototype of unventilated solar drier used in this study was designed and made by LENREZA.

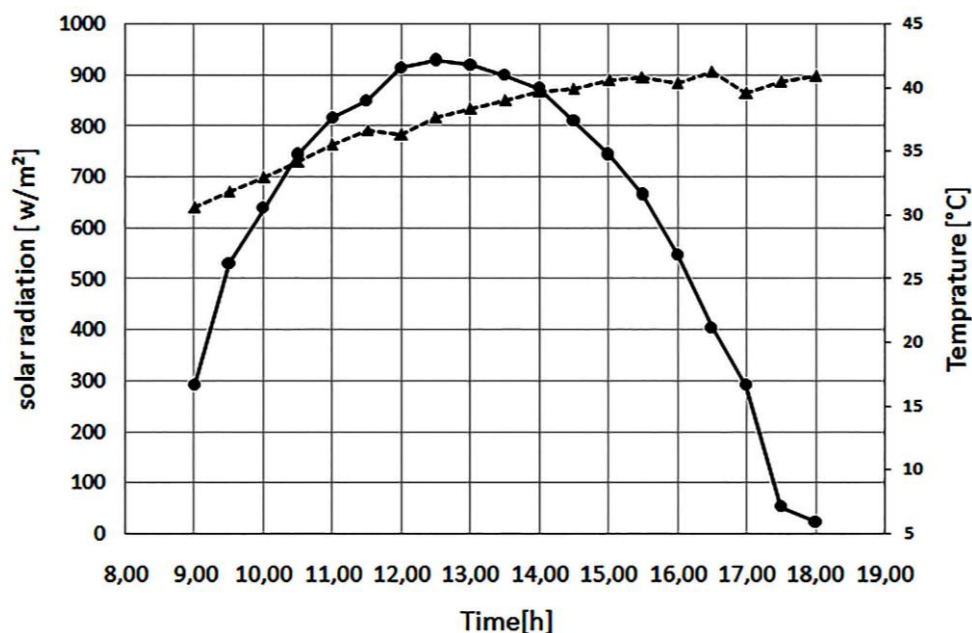


**Fig. 1.** Typical daily solar radiation and ambient temperature variations in Ouargla city (May 2015)

The prototype of unventilated solar drier used in this study was designed and made by LENREZA laboratory, Ourgla University in Algeria.

The experimental procedures consist of the following steps.

- i. Preparation of the solar collectors (Adaptation of angle, Position...).
- ii. Installation of the measuring devices.
- iii. Conducting the experiments with acquisition software.
- iv. Recording measurements every 15 minutes by the data acquisition system (the outlet air temperature of the collector, the inlet air temperature, the ambient air temperature, incident solar radiation on the collector and wind speed near the collector)

The experimental protocol is conducted by measuring the daily temperature in the collectors, solar radiation and wind speed, between 9h and 17h local time.

For the purpose of reducing the heat loss, both collectors are covered at the bottom in an insulating material. Furthermore, the absorber of both collectors is coated in a black layer of material that has a high solar radiation absorptance and low infrared ray emittance to maximize the absorption of solar radiation.

In order to investigate separately the efficiency of both simple pass collector and double pass collector, two different experimental protocols have been carried out. In the first protocol, the simple pass and the double pass collectors are not connected with the chamber as shown in Figure 2(a) and

2(b), whereas in the second one, both collectors are connected with the drying chamber as illustrated in Figures 3(a) and 3(b). The first part of the experiment was conducted from April 6th to April 15th, 2015, whereas, the second one was done from December 29th, 2015 to January 2nd, 2016. The efficiency of both collectors is calculated using Letz equation [20].



Length: 2 m . Width: 1 m. Thickness: 0.08 m/0.16 m. Absorber: plat aluminum painted in black+ the sand dunes. Insulation: polystyrene. Angle of orientation: 32°



Length: 2 m . Width: 1 m. Thickness: 0.13 m. 1st passage:0.065 m. 2nd passage:0.065 m. absorber: plate aluminum. Insulation: Glass wool. Orientation angle: 32°

**Fig. 2.** Geometric configuration of collectors (a) simple pass and (b) double pass



Length of collector: 2 m. Width: 1 m. Thickness: 0.055 m  
 Depth of chamber: 0.7 m Length of chamber: 0.87 m.  
 Width of chamber: 0.68. Absorber: plate aluminum.  
 Insulation: Polystyrene. Angle of orientation: 31°



Length of collector: 2.53 m. Width: 1 m. Thickness: 0.13 m  
 1st passage: 0.065 m. 2nd passage: 0.065 m. Depth of chamber: 0.7 m Length of chamber: 0.87 m. Width of chamber: 0.68. Absorber: plate aluminum. Insulation: Polystyrene. Angle of orientation: 32°

**Fig. 3.** Laboratory scale solar drier connected to the collector; (a) simple pass and (b) double pass

## 2.2 Simulation Part

### 2.2.1 Governing equations

The analysis of thermo-aerodynamics phenomena requires a great number of parameters such as the geometry of the collector, characteristics of the used materials and the physical parameters (temperature, air velocity) as well as the geometry of the drying chamber [18]. The following assumptions were made in order to simplify the calculation

- The flow is assumed to be two-dimensional.
- The fluid is assumed to be a Newtonian and incompressible.
- Viscous dissipations are neglected
- All properties of the air are constant except for the density in buoyancy force.

For constant flow, equations of continuity, energy and momentum are written as follows [21,22]

#### Continuity equation

$$\frac{\partial u}{\partial x} + \frac{\partial v}{\partial y} = 0 \quad (1)$$

#### Momentum conservation equation

$$u \frac{\partial u}{\partial x} + v \frac{\partial u}{\partial y} = -\frac{1}{\rho_0} \frac{\partial p}{\partial x} + v \left( \frac{\partial^2 u}{\partial x^2} + \frac{\partial^2 u}{\partial y^2} \right) - g\beta(T - T_c)\cos\theta \quad (2)$$

$$u \frac{\partial v}{\partial x} + v \frac{\partial v}{\partial y} = -\frac{1}{\rho_0} \frac{\partial p}{\partial y} + v \left( \frac{\partial^2 v}{\partial x^2} + \frac{\partial^2 v}{\partial y^2} \right) - g\beta(T - T_c)\sin\theta$$

#### Energy conservation equation

$$u \frac{\partial T}{\partial x} + v \frac{\partial T}{\partial y} = \alpha \left( \frac{\partial^2 T}{\partial x^2} + \frac{\partial^2 T}{\partial y^2} \right) \quad (3)$$

### 2.2.2 Initial and boundary conditions

#### Initial condition

$$\text{at } t = 0 \quad \begin{cases} u(0, y, 0) = u_{int} \cdot \cos\theta \\ v(0, y, 0) = u_{int} \cdot \sin\theta \\ T = T_a \end{cases} \quad (4)$$

#### Inlet boundary conditions

$$\begin{cases} u(0, y, t) = u_{int} \cdot \cos\theta \\ v(0, y, t) = u_{int} \cdot \sin\theta \\ T = T_a \end{cases} \quad (5)$$

#### Outlet boundary conditions

$$\begin{cases} \left. \frac{dT}{dx} \right|_{(0,y,t)} = 0 \\ P = P_{atm} \end{cases} \quad (6)$$



### Wall boundary conditions

$$-\lambda_v \frac{dT}{dy} = h_a(T(x, H, t) - T_a) + \varepsilon\sigma(T^4(x, H, t) - T_s^4) + I \quad (7)$$

### 2.2.3 Numerical procedures

These equations are solved by using a fluid dynamic code which is based on the finite volume method (FVM). In this part of the study, a simulation of the prototype of the indirect solar dryer (Figure 3(a)), using fluent software in 2D configuration, is done with the measured data based on the climatic conditions at the collector inlet (temperature and velocity). The computation starts first by validating the model of simulation through a comparison between the measured temperature in three different positions inside the chamber with the data obtained from the simulation as shown in Figure 6, and then, the effects of various parameters including, the length and width of the simple pass collector are investigated in order to enhance the homogeneity of the temperature distributed inside the drying chamber.

## 3. Results and Discussion

In this section, the obtained results related to the efficiency of both the simple pass and double pass solar collectors are first discussed. In the second part, the focus is on the computed results in order to determine the optimal geometric parameters that could result in a homogeneous distribution of temperature which helps in preventing the degradation of product inside the drying chamber.

Figure 4 delineates the variations in the efficiency and  $\Delta T$  (the gradient of temperature between the inlet and outlet of the collector) of both the simple pass and double pass collectors with respect to the daily operating time.

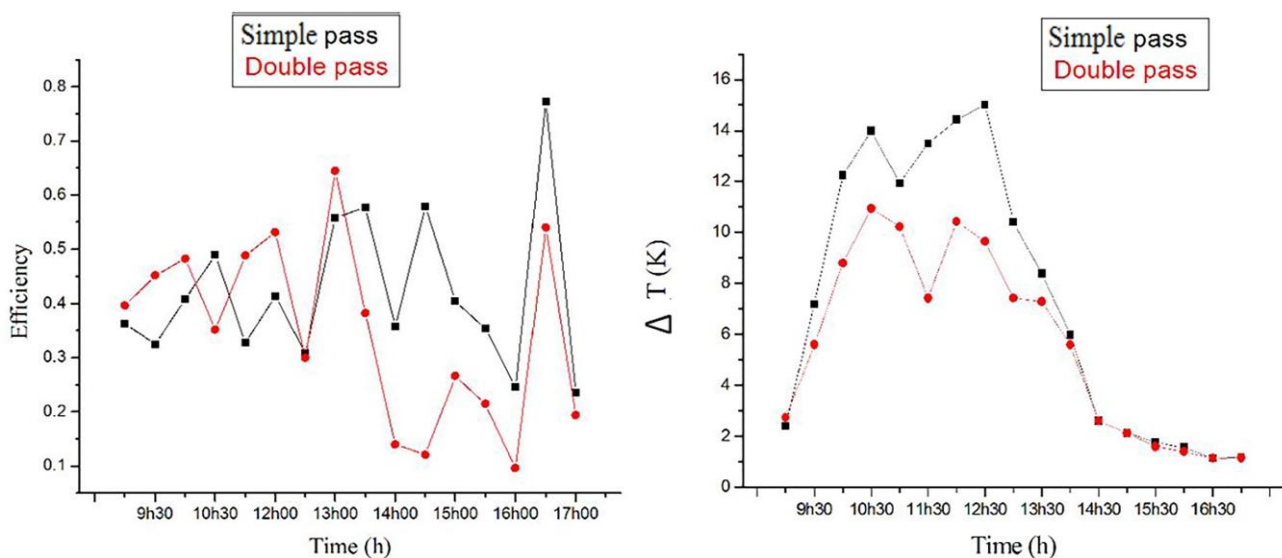


**Fig. 4.** The efficiency of collectors without being connected with the drying chamber

It can be noticed that the efficiency of the air collectors (the simple pass and double pass) strongly depends on the gradient of temperature  $\Delta T$  which increases regularly until 14h and then starts to go

down. Moreover, from 14h to 17h the efficiency of the simple pass collector is higher in value in comparison with that of the double pass collector

Thus, it can be concluded that the simple pass collector is more efficient on average by 8% than the double pass collector because it can absorb and store a greater quantity of solar radiation during the operating time.

Figure 5 represents the efficiency values of the simple pass collectors when connected with the drying chamber, and shows a higher efficiency than that noticed in the first set of experiments because of the high gradient of temperature  $\Delta T$  ( $\Delta T$  from 35°C to 40°C). Additionally, the curve has a sinusoidal form resulting fundamentally from a decrease in the air velocity which becomes almost nil at the inlet of the collector.

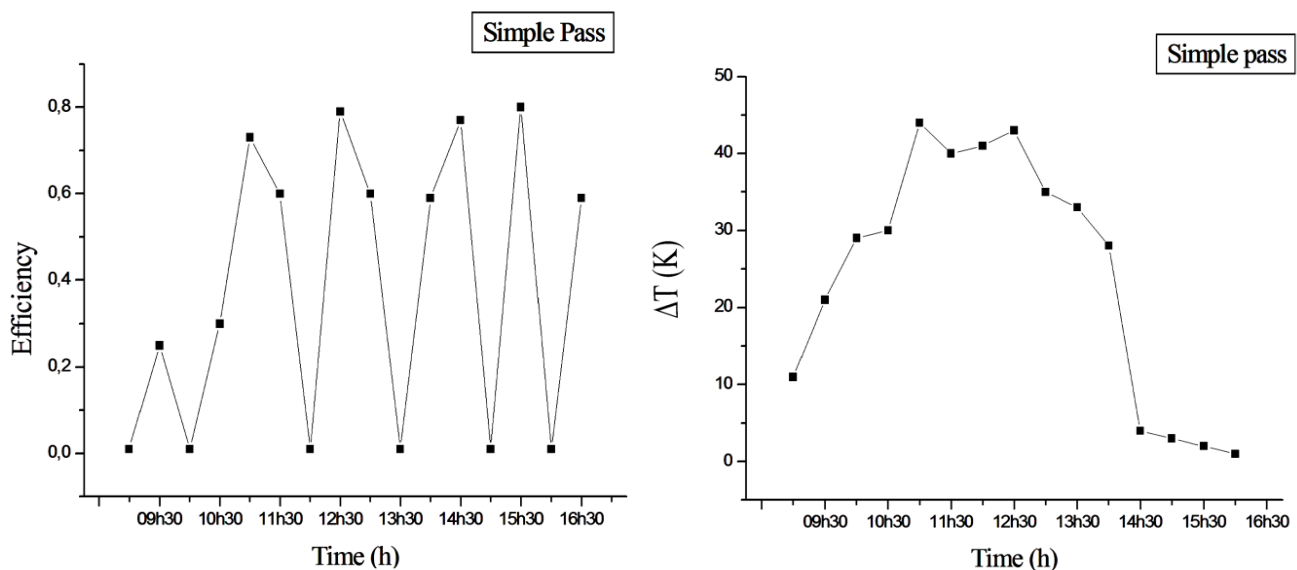
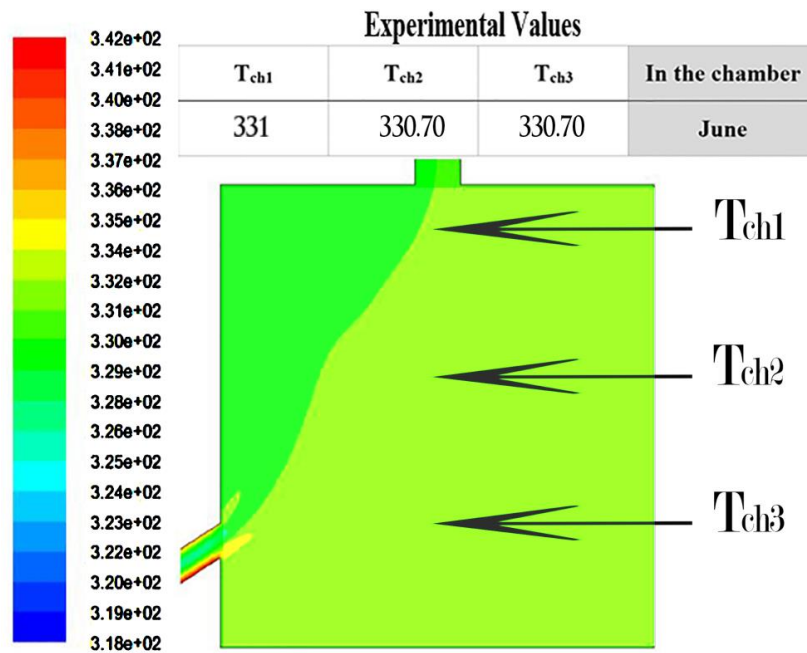


Fig. 5. The efficiency of the simple pass collector when connected with the drying chamber

### 3.1 Validation of Model

Before examining the influence of length, width of the selected collector (simple pass collector) on the thermal behavior in drying system, the developed numerical CFD model is validated with experimental data culled from literature under the same operating conditions [18,23,24]. Figure 6 shows the numerical results of temperature distributed inside the drying chamber. Despite, the small margin of error (2-3°C) which is often acceptable in practical situations, an agreement between the simulated and experimental values is reached.



**Fig. 6.** Comparison between the simulated and experimental temperatures inside the drying chamber

### 3.2 Simulation of Unmodified Air Collector

The experimental data collected during several months (April, May, June, and November) in Ouargla city, which are summarized in Table 1, are considered as input data in the numerical model. This data is characterized by moderate and low inlet air velocity corresponding respectively to 0.8 m/s and 0.16-0.17 m/s. The first was recorded on April-May 2015, and the second one on November 2010 and June 2011 as shown in this table.

**Table 1**

Boundary conditions taken as input data in the numerical model

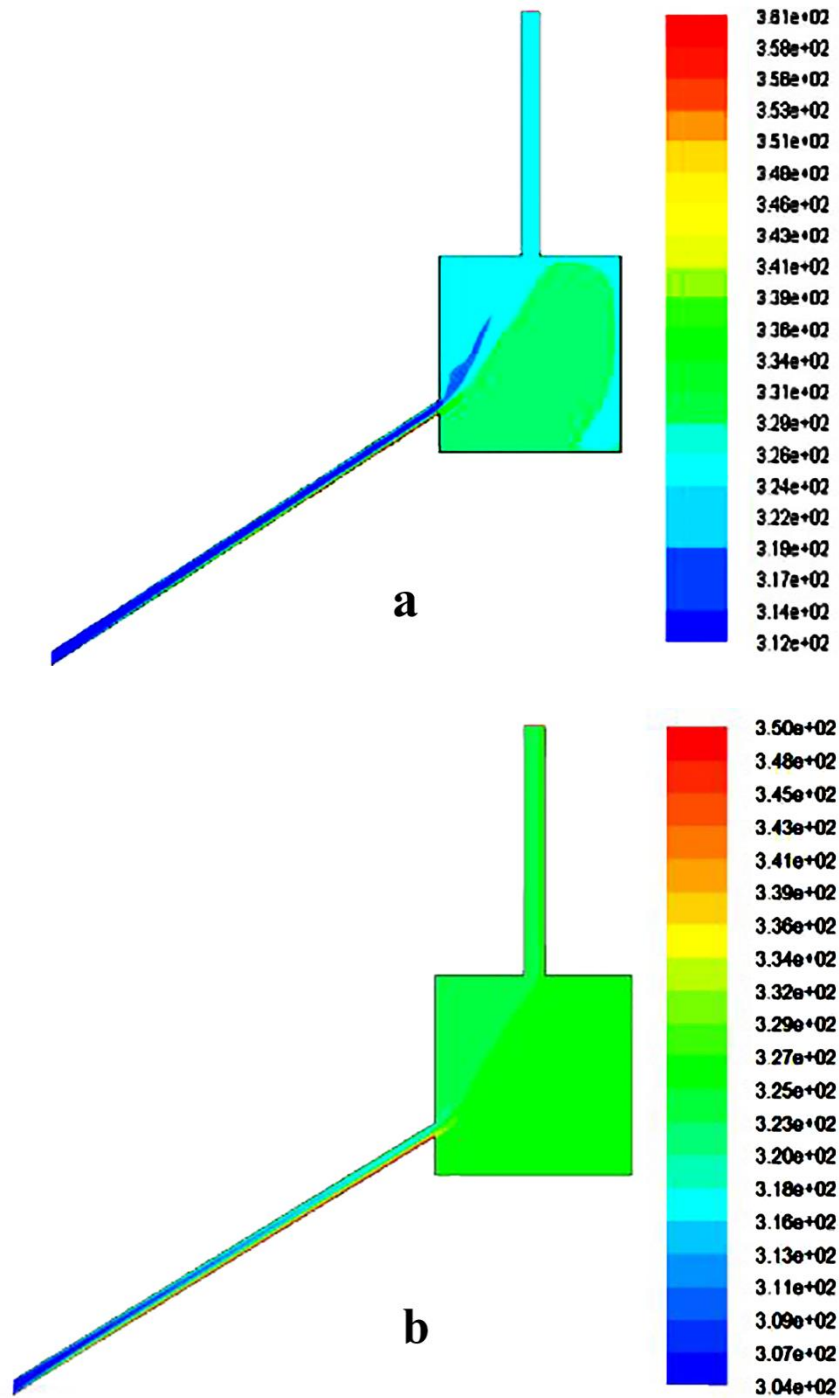
| Day                             | $V_e$ (m/s) | $T_e$ (K) | $T_{abs}$ (K) | $T_v$ (K) | $T_s$ (K) |
|---------------------------------|-------------|-----------|---------------|-----------|-----------|
| April, 28 <sup>th</sup> , 2015  | 0.8         | 313.4     | 376.3         | 346.8     | 345.8     |
| May, 04 <sup>th</sup> , 2015    | 0.8         | 311.8     | 375.8         | 347.5     | 354.9     |
| June 25 <sup>th</sup> , 2011    | 0.16        | 318       | 342           | 337.3     | 335       |
| November 2 <sup>nd</sup> , 2010 | 0.17        | 304.3     | 354.1         | 328.8     | 322.5     |

Figure 7 illustrates the numerical data and temperature distributed inside the drying chamber where two annotations are worth mentioning. Firstly, for the days with moderate inlet air velocity, a significant stratification phenomenon of temperature is clearly apparent in Figure 7(a). Secondly, in Figure 7(b), corresponding to climatic conditions characterized with low inlet air velocity, a low temperature stratification compared to previous results can be noticed.

The curve representing the longitudinal rise in temperature inside the solar collector in three different positions respectively: under glass, above the absorber and at the center are all depicted in Figure 8. When the inlet air velocity is moderate, three different phases are shown according to the central position; the rise in temperature at the center with respect to length is flat in the first phase from the inlet to 0.8 m. Beyond this distance a slight increase in temperature which is about 1.35°C when 1.6 m in length is reached. However, the temperature increases significantly at the outlet, which explains the build-up of heat inside the collector. Whereas, in Figure 8(b), a fast increase in



temperature at the center can be observed as expected in such physical condition due to the low inlet air velocity leading to a homogeneous temperature distributed inside the drying chamber.



**Fig. 7.** Simulated temperature distributed inside the drying system (air collector-drying chamber): (a) moderate inlet air velocity (0.8 m/s) and (b) low inlet air velocity (0.16 m/s)

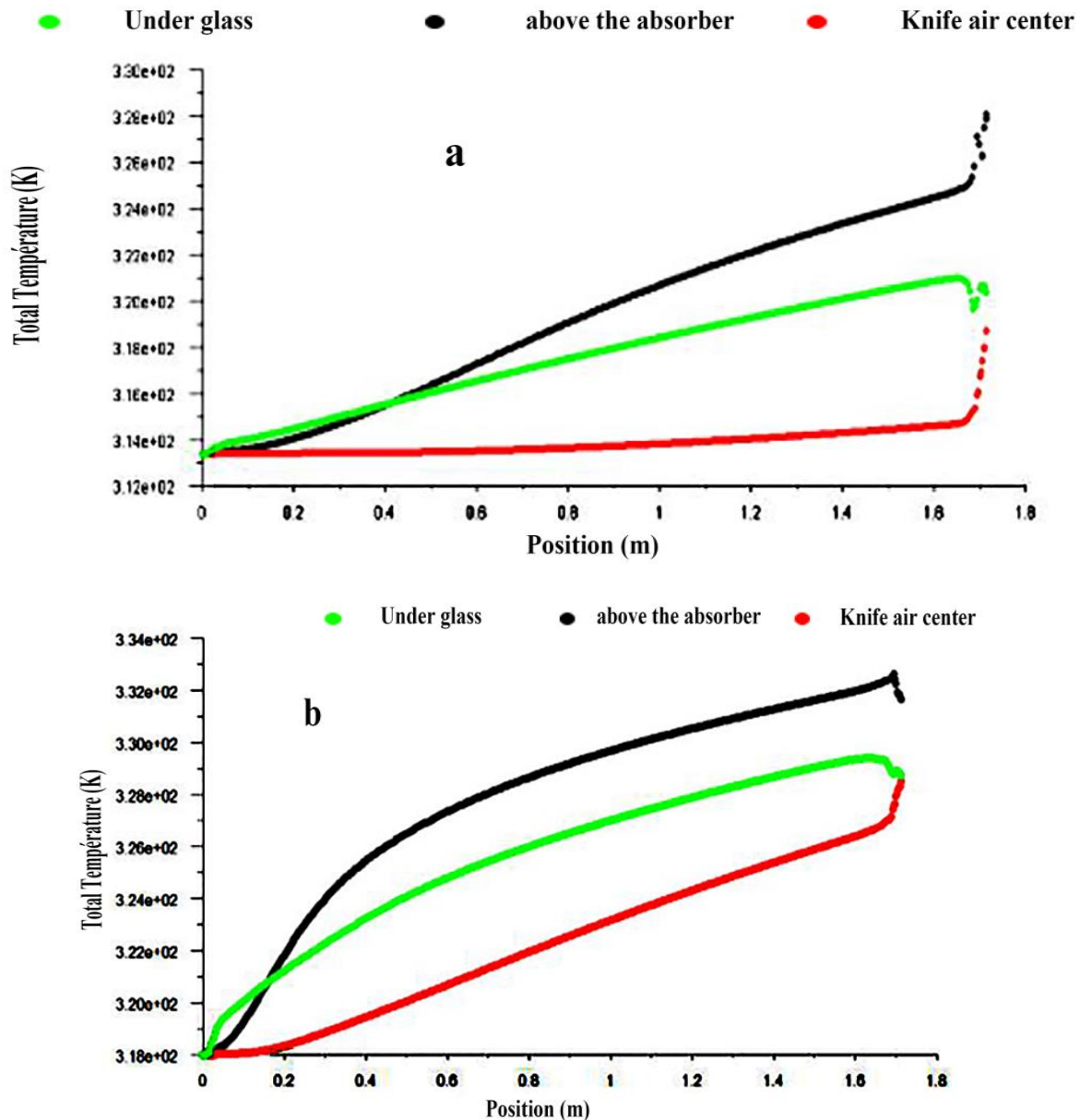


**Fig. 8.** Longitudinal rise in temperature in three different positions inside the air collector (a) moderate inlet air velocity (0.8 m/s) and (b) low inlet air velocity (0.16 m/s)

### 3.3 Simulation of Modified Solar Air Collector

In this part, we examine the effect of the modified width and length of the collector at both moderate and low inlet air velocity. Figure 9 gives a schematic view of the changes.

Figure 10 illustrates the distribution of temperature inside the drying chamber when the modified collector length is either 4m or 6m and the width is 1 m at moderate inlet air velocity. In Figure 10(a), the modified length is 4m resulting in a homogeneous distribution of temperature except in the vicinity of the southern side where a small increase in temperature of 2°C is noted. Whereas Figure 10(b) shows that the temperature of air at the collector outlet is more elevated by 329K when the length is six meters. However, the distribution of the temperature in the drying chamber is not uniform. It is worth mentioning that the lack of homogeneity, which is  $\Delta T=9K$ , results from the build-up of heat throughout the collector.

Figure 11(a) delineates the obtained results of air temperature in 3D inside the dry chamber after modifying the width of collector (the length is 2 m) at moderate inlet air velocity. When the width is 1.5m, the temperature of outlet air goes up by 9K (Figure 11(a)) due to an increase in the rate of air flow. However, the distribution of temperature in the drying chamber remains less homogeneous. The same results were obtained with the tow meter collector in width as shown in Figure 11(b).

Similar calculations were made at low inlet air velocity with the same geometric modifications that are mentioned above. The obtained results indicate that for all geometric modifications there is a good homogeneity of temperature distributed inside the chamber ranging from 330K to 335K as shown in Figure 12, except when the length of collector is 6 m because the temperature reaches 346K, which could affect negatively the quality of the dried product.

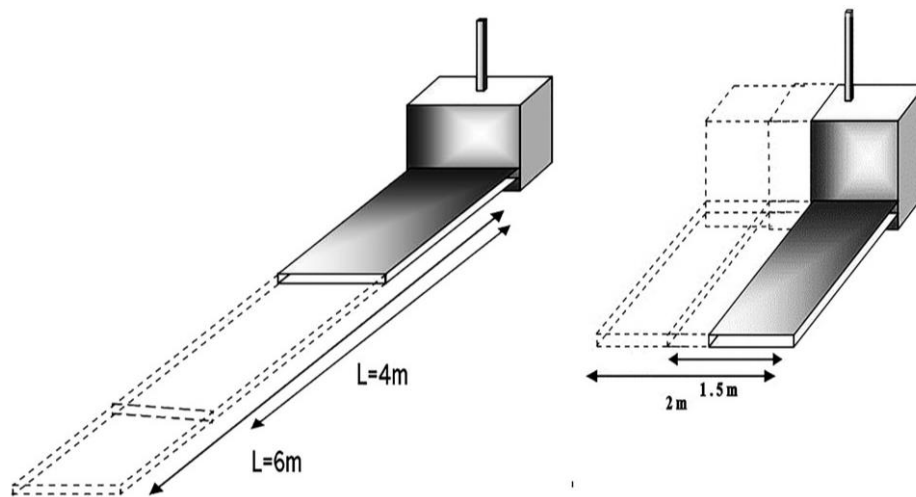


Fig. 9. Modification of width and length of collector

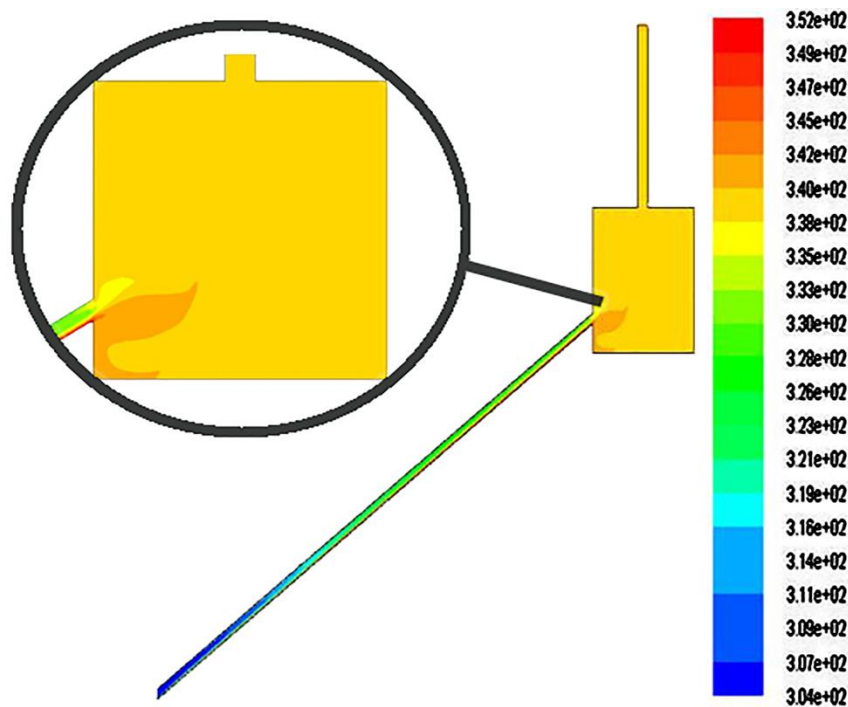
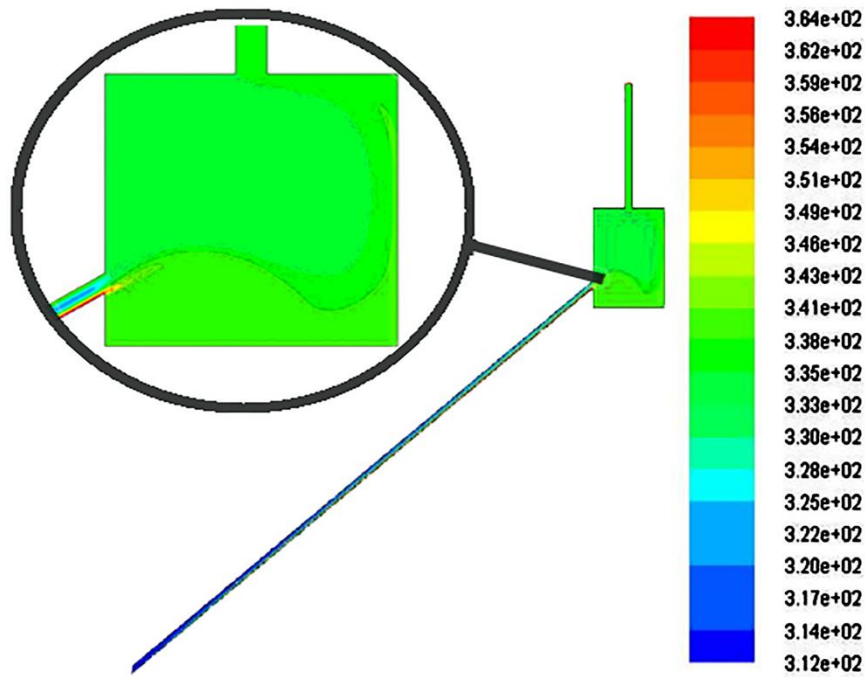
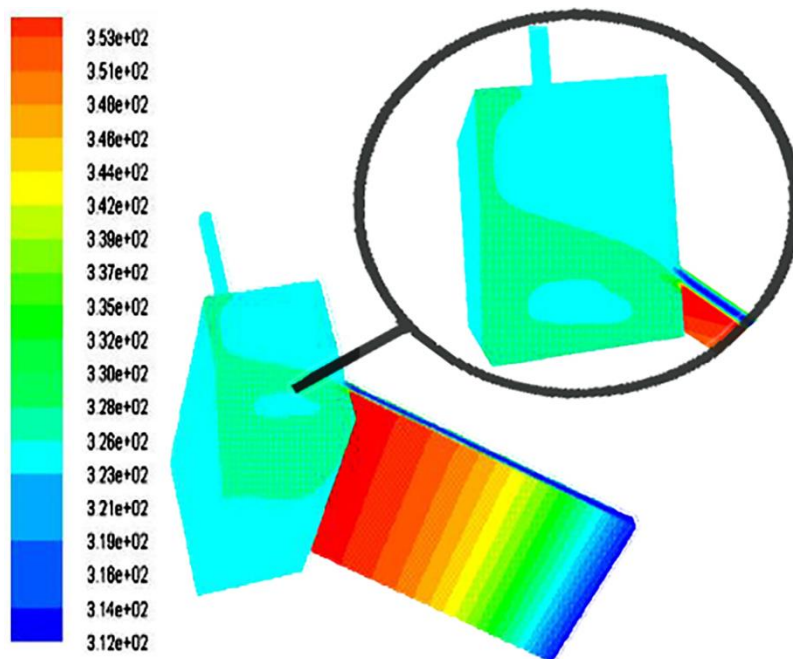


Fig. 10. (a) Simulation results when the length is modified  $L=4m$  (the width  $l=1m$ ) at moderate inlet air velocity



**Fig. 10.** (b) Simulation results when the length is modified  $L=6\text{m}$  (the width  $l=1\text{m}$ ) at moderate inlet air velocity



**Fig. 11.** (a) 3D Simulation results at moderate velocity when the width is 1.5m (the length  $L= 2\text{m}$ )

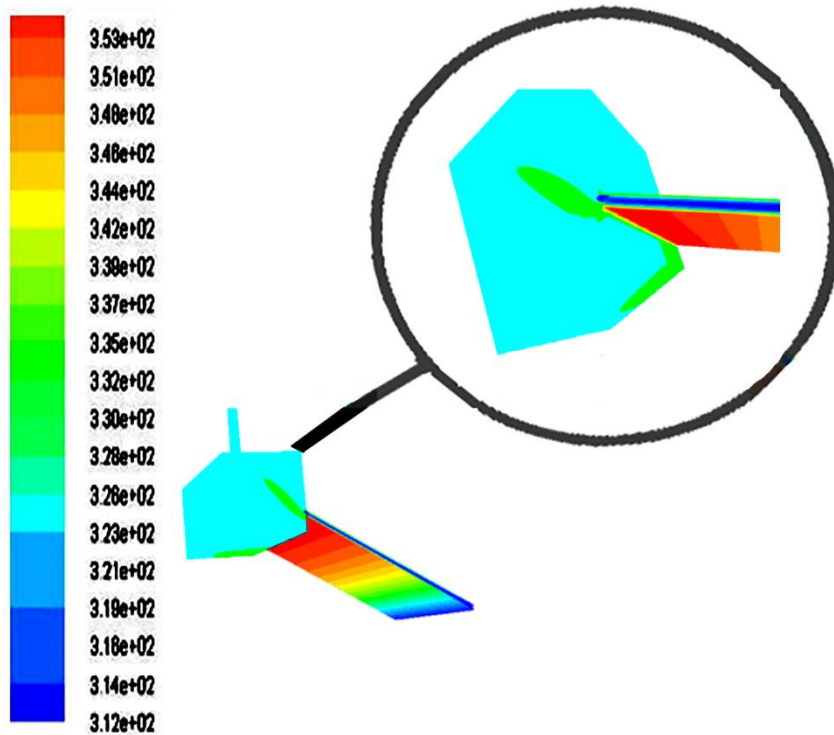


Fig. 11. (b) 3D Simulation results at moderate velocity when the width is 2m (the length  $L=2m$ )

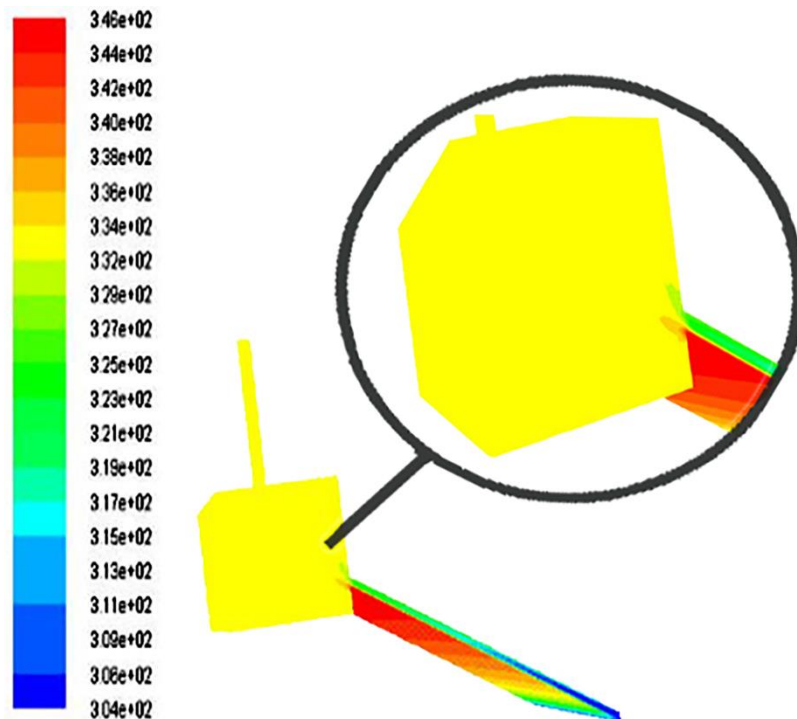


Fig. 12. 3D Simulation results at low velocity when the width  $l=1.5m$  and the length  $L=2m$

#### 4. Conclusion

In this paper, the influence of the geometric parameters including the length and width of the solar flat plate collectors on the distribution of temperature inside the drying chamber was



numerically investigated under the climatic conditions of Ouargla city (Algeria). In terms of collector efficiency, experimental measurements on both the simple pass and double pass collectors were carried out. The findings show that the simple pass collector is on average 8% more efficient than the double pass collector. Several numerical tests using a CFD software were performed at moderate and low inlet air velocity on the prototype of solar indirect unventilated drying system, which is composed of the simple pass collector connected with the drying chamber. The obtained results indicate that the distribution of temperature in the drying chamber is less homogeneous in both cases. In addition, the gradient of temperature between the inlet and outlet of collector is much lower when the inlet air velocity is moderate whereas it is higher when the inlet air velocity is low.

After investigating carefully, the effect of the length and width of collector on the homogeneity of temperature at different inlet air velocity, the following geometric configuration, which is 04 meters in length and 1.5 meters in width, seems to be the best option to achieve the appropriate degree of temperature with a good homogeneity regardless of the inlet air velocity.

### Acknowledgments

The experimental part of this work was carried out at the Laboratory for the Development of New and Renewable Energies in Arid Zones (LENREZA) and the numerical calculation was performed at the Laboratory of Mechanics, Physics and Mathematical Modeling of Medea University. The authors would like to show their gratitude for their assistance.

### References

- [1] Bennamoun, Lyes. "Integration of photovoltaic cells in solar drying systems." *Drying Technology* 31, no. 11 (2013): 1284-1296.
- [2] Zomorodian, A. A., and M. Dadashzadeh. "Indirect and mixed mode solar drying mathematical models for sultana grape." (2009): 391-400.
- [3] Cerci, Kamil Neyfel, and Ebru Kavak Akpınar. "Experimental determination of convective heat transfer coefficient during open sun and greenhouse drying of apple slices." *J. Therm. Eng* 2 (2016): 741-747.
- [4] Noh, Arina Mohd, Sohif Mat, and Mohd Hafidz Ruslan. "CFD simulation of temperature and air flow distribution inside industrial scale solar dryer." *Journal of Advanced Research in Fluid Mechanics and Thermal Sciences* 45, no. 1 (2018): 156-164.
- [5] Sreekumar, A., P. E. Manikantan, and K. P. Vijayakumar. "Performance of indirect solar cabinet dryer." *Energy Conversion and Management* 49, no. 6 (2008): 1388-1395.
- [6] Fudholi, Ahmad, Kamaruzzaman Sopian, Mohd Hafidz Ruslan, M. A. Alghoul, and M. Y. Sulaiman. "Review of solar dryers for agricultural and marine products." *Renewable and Sustainable Energy Reviews* 14, no. 1 (2010): 1-30.
- [7] Bennamoun, Lyes. "Reviewing the experience of solar drying in Algeria with presentation of the different design aspects of solar dryers." *Renewable and Sustainable Energy Reviews* 15, no. 7 (2011): 3371-3379.
- [8] Sharma, Atul, C. R. Chen, and Nguyen Vu Lan. "Solar-energy drying systems: A review." *Renewable and Sustainable Energy Reviews* 13, no. 6-7 (2009): 1185-1210.
- [9] VijayaVenkataRaman, S., S. Iniyar, and Ranko Goic. "A review of solar drying technologies." *Renewable and Sustainable Energy Reviews* 16, no. 5 (2012): 2652-2670.
- [10] Misha, Suhaimi, Sohif Mat, Mohd Hafidz Ruslan, Elias Salleh, and Kamaruzzaman Sopian. "A Study of Drying Uniformity in a New Design of Tray Dryer." *Journal of Advanced Research in Fluid Mechanics and Thermal Sciences* 52, no. 2 (2018): 129-138.
- [11] Stegou-Sagia, A., and D. V. Fragkou. "Thin layer drying modeling of apples and apricots in a solar-assisted drying system." *Journal of Thermal Engineering* 4, no. 1 (2018): 1680-1691.
- [12] Jain, Dilip. "Modeling the system performance of multi-tray crop drying using an inclined multi-pass solar air heater with in-built thermal storage." *Journal of food engineering* 71, no. 1 (2005): 44-54.
- [13] Choicharoen, Kwanchai, Sakamon Devahastin, and Somchart Soponronnarit. "Numerical simulation of multiphase transport phenomena during impinging stream drying of a particulate material." *Drying Technology* 30, no. 11-12 (2012): 1227-1237.
- [14] Sikula, Ondrej, Josef Plasek, and Jiri Hirs. "The effect of shielding barriers on solar air collector gains." *Energy Procedia* 36 (2013): 1070-1075.

- [15] Ghaderian, J., C. N. Azwadi, and H. Mohammed. "Modelling of energy and exergy analysis for a double-pass solar air heater system." *J. Adv. Res. Fluid Mech. Therm. Sci* 16, no. 1 (2015): 15-32.
- [16] Suwasti, S., S. Abadi, and A. M. Shiddiq Yunus. Jamal. "Impacts of fin variation on the performance of shelf type solar dryer." *Journal of Advanced Research in Fluid Mechanics and Thermal Sciences* 13, no. 1 (2015): 17-21.
- [17] Karim, M. A., and MiNAr Hawlader. "Development of solar air collectors for drying applications." *Energy Conversion and Management* 45, no. 3 (2004): 329-344.
- [18] A. Babahani, D. Halassa, A. Boubekri, D. Mennouche, H. Belahia, Proc. Du 5ème Séminaire Maghrébin sur les Sciences et les Technologies du Séchage, Ouargla - Algeria, (2015): 419-424.
- [19] Bouchahm, Yasmina, Fatiha Bourbia, and Azeddine Belhamri. "Performance analysis and improvement of the use of wind tower in hot dry climate." *Renewable Energy* 36, no. 3 (2011): 898-906.
- [20] Abene, A., V. Dubois, M. Le Ray, and A. Ouagued. "Study of a solar air flat plate collector: use of obstacles and application for the drying of grape." *Journal of Food Engineering* 65, no. 1 (2004): 15-22.
- [21] Patankar, S. V. "Numerical Heat Transfer and Fluid Flow (Series in Computation and Physical Processes in Mechanics and Thermal Sciences)." (1980).
- [22] N.C. Markatos and K.A. Pericleous. "Turbulent Laminar and natural convection in year enclosed cavity." *Int. J. Heat Farmhouse Transfer* 27, no. 5 (1984): 755-772.
- [23] D. Halassa, A. Arbia, O. Chaoubi, A. Boubekri, M. Announ, H. Belahya, Proc. of 5ème Séminaire Maghrébin sur les Sciences et les Technologies du Séchage, Ouargla-Algeria, (2015): 82-86.
- [24] D. Halassa, I. Hendaoui, B. Regagda, A. Boubekri, M. Announ, D. Mennouche, Proc. of 5ème Séminaire Maghrébin sur les Sciences et les Technologies du Séchage, Ouargla-Algeria, (2015): 401-406.